

Water/Ethanol Displacement Reactions in Vanadyl Phosphate

Ludvík Beneš,^{*,[a]} Klára Melánová,^[a] Miroslava Trchová,^[b] Pavla Čapková,^[b]
and Pavel Matějka^[c]

Keywords: Intercalations / Vanadyl phosphate / Ethanol / Hydration / Kinetics

The course of the replacement of ethanol by water molecules in the $\text{VOPO}_4 \cdot 2\text{C}_2\text{H}_5\text{OH}$ intercalate, and of water by ethanol in $\text{VOPO}_4 \cdot 2\text{H}_2\text{O}$ has been studied by X-ray diffraction and infrared and Raman spectroscopy. Formation of mixed phase $\text{VOPO}_4 \cdot \text{C}_2\text{H}_5\text{OH} \cdot \text{H}_2\text{O}$ was not observed. The shape of the kinetics curves indicates a transition of at least one reaction zone through the crystal. A delay in formation of the product

in comparison with the decrease in the amount of starting material can be explained by the existence of non-diffracting advancing phase boundary. In a VOPO_4 /ethanol/water system, $\text{VOPO}_4 \cdot 2\text{C}_2\text{H}_5\text{OH}$ is formed as the only product when the system contained more than 96 vol% of ethanol, whereas in the system with less than 94 vol% of ethanol only $\text{VOPO}_4 \cdot 2\text{H}_2\text{O}$ is present.

Introduction

Compounds based on vanadyl phosphate are of great interest because of their catalytic properties for oxidation. The structure of vanadyl phosphate dihydrate, $\text{VOPO}_4 \cdot 2\text{H}_2\text{O}$, has been determined by Tietze using X-ray diffraction^[1] as tetragonal, space group $P4/nmm$, $a = 6.202$ Å and $c = 7.410$ Å. Tachez et al.^[2] used neutron powder diffraction of the deuterated compound in order to determine the positions of hydrogen atoms and determined the space group $P4/n$, $a = 6.215$ Å and $c = 7.403$ Å. The layers are built up of PO_4 tetrahedra linked to distorted VO_6 octahedra by sharing four equatorial oxygen atoms. VO_6 octahedra are completed by axial oxygens, one of which is a vanadyl oxygen, and the second of which belongs to the interlayer water molecule coordinated to vanadium. The second water molecule is bonded by weak H-bridges between the VOPO_4 layers.

Vanadyl phosphate is a good host structure for intercalation of organic molecules with suitable functional groups.^[3] Intercalation compounds of vanadyl phosphate with aliphatic and aromatic amines,^[4–6] heterocycles,^[7] alcohols and diols,^[8] carboxylic acids^[9] and their amides^[10] have been studied. From this point of view, vanadyl phosphate dihydrate can be regarded as an intercalate of α_1 - VOPO_4 with water.

The time course of intercalation of water into α_1 - VOPO_4 has been followed by TMA, XRD^[11] and infrared and Raman spectroscopy.^[12] Formation of vanadyl phosphate monohydrate was not observed during hydration of the an-

hydrous form under ambient conditions. Instead, the broadening and the shift of positions of the (00 l) diffraction lines were observed. These phenomena were explained by formation of a Hendricks–Teller disordered layered structure, which is composed of the α_1 - VOPO_4 and $\text{VOPO}_4 \cdot 2\text{H}_2\text{O}$ layers. The vanadyl stretching band appears to be especially sensitive to atoms coordinated to the vanadium within an octahedral arrangement in the host lattice structure. During the intercalation, the position of this band at 1035 cm^{-1} in the anhydrous form changes to 995 cm^{-1} , which are typical values for mono- and dihydrates. The additional peak at 1017 cm^{-1} occurring in the initial stages of intercalation was explained in terms of a random stacking of intercalated and non-intercalated layers in the sample.

Ethanol can be intercalated into anhydrous vanadyl phosphate^[13] or it can replace the water molecules in $\text{VOPO}_4 \cdot 2\text{H}_2\text{O}$.^[8] The kinetics of intercalation of ethanol into anhydrous vanadyl phosphate were studied by XRD and a volumetric method, and the kinetics curves obtained were found to have a sigmoidal shape.^[14] During intercalation, the original host and the intercalate are present in one crystal. Both phases are separated by an advancing phase boundary.^[15] A molecular mechanics simulation, combined with X-ray diffraction and supported by vibrational spectroscopy, was used to investigate the layered structure of vanadyl phosphate VOPO_4 intercalated with ethanol.^[16] The bilayer arrangement of ethanol molecules in the interlayer was found, giving the calculated basal spacing $d = 13.21$ Å; the experimental d value obtained from X-ray diffraction is 13.17 Å. One half of the total number of $\text{CH}_3\text{CH}_2\text{OH}$ molecules is anchored by their oxygen to VOPO_4 layers to complete the vanadium octahedra and their orientation is not very strictly defined. The second half of the ethanol molecules are linked by hydrogen bonds to the anchored ethanol and sometimes also to the layer oxygen. The position and orientation of this anchored ethanol with respect to VOPO_4 layers exhibits a certain degree of disorder, resulting in the disorder in the layer stacking.

[a] Joint Laboratory of Solid State Chemistry of the Academy of Sciences of the Czech Republic and University of Pardubice, Studentská 84, 532 10 Pardubice, Czech Republic
Fax: (internat.) + 420-40/6036011
E-mail: ludvik.benes@upce.cz

[b] Faculty of Mathematics and Physics, Charles University, Ke Karlovu 3, 121 16 Prague, Czech Republic

[c] Department of Analytical Chemistry, Institute of Chemical Technology, Technická 5, 166 28 Prague, Czech Republic

Owing to the instability of $\text{VOPO}_4 \cdot 2\text{C}_2\text{H}_5\text{OH}$ when exposed to air, the water molecules intercalate into this system at room temperature by simply keeping the compounds under ambient conditions. The course of reintercalation of water molecules into vanadyl phosphate intercalate with ethanol was studied by X-ray diffraction and infrared and Raman spectroscopy. The aim of this work is to contribute to the elucidation of the mechanism of water/ethanol displacement in vanadyl phosphate.

Results and Discussion

X-ray Study

In order to study an equilibration in a VOPO_4 /ethanol/water system, $\text{VOPO}_4 \cdot 2\text{H}_2\text{O}$ was contacted with ethanol containing a known amount of water. The dependence of the basal spacing of solid products on the concentration of ethanol is shown in Figure 1. It is evident that only two phases are formed in this system. A mixture of $\text{VOPO}_4 \cdot 2\text{C}_2\text{H}_5\text{OH}$ and $\text{VOPO}_4 \cdot 2\text{H}_2\text{O}$ phases is formed in the ethanol/water solvent containing from 94 to 96 vol% of ethanol. Above 96 vol% of ethanol, only $\text{VOPO}_4 \cdot 2\text{C}_2\text{H}_5\text{OH}$ (basal spacing 13.17\AA) is present, whereas below 94 vol% of ethanol in the solvent mixture only $\text{VOPO}_4 \cdot 2\text{H}_2\text{O}$ (7.41\AA) is formed. These results were obtained from the properties of the binary alcohol/water mixture, where an azeotrope with 96 vol% of ethanol is formed as a mixture with the most stable structure. Ethanol containing a lower content of water is hygroscopic and tends to take up water. Therefore, water is taken from $\text{VOPO}_4 \cdot 2\text{H}_2\text{O}$ and the water molecules in the interlayer space are replaced by ethanol molecules. The solvent with more than 6% of water, on the other hand, can provide water molecules to replace ethanol in $\text{VOPO}_4 \cdot 2\text{C}_2\text{H}_5\text{OH}$ and leads to the formation of $\text{VOPO}_4 \cdot 2\text{H}_2\text{O}$. This means that the co-intercalate $\text{VOPO}_4 \cdot \text{C}_2\text{H}_5\text{OH} \cdot \text{H}_2\text{O}$ containing molecules of ethanol and water together was not observed. The co-intercalate of this type was reported by Matsubayashi as a starting material for the intercalation of ferrocene into VOPO_4 .^[17] Practically the same result is obtained when $\text{VOPO}_4 \cdot 2\text{C}_2\text{H}_5\text{OH}$ is contacted with ethanol/water mixtures.

In situ X-ray diffraction was employed to follow the reaction of polycrystalline $\text{VOPO}_4 \cdot 2\text{H}_2\text{O}$ with ethanol vapors. The lines observed in the diffractograms belong to either vanadyl phosphate dihydrate or ethanol-intercalated vanadyl phosphate, indicating that there is no intermediate product such as $\text{VOPO}_4 \cdot \text{C}_2\text{H}_5\text{OH} \cdot \text{H}_2\text{O}$. In the region investigated, four sharp (00 l) lines of the intercalate were observed, which gave the same value for the basal spacing. The interlayer distances calculated from the (00 l) reflections of both phases remain constant. Small changes of line-widths during reintercalation can be explained by a decrease in the size of an area of the dihydrate and an increase in the size of an area of the intercalate formed in the crystals. It can be assumed from the XRD results that the intercalate is formed directly in the majority of the crystals,

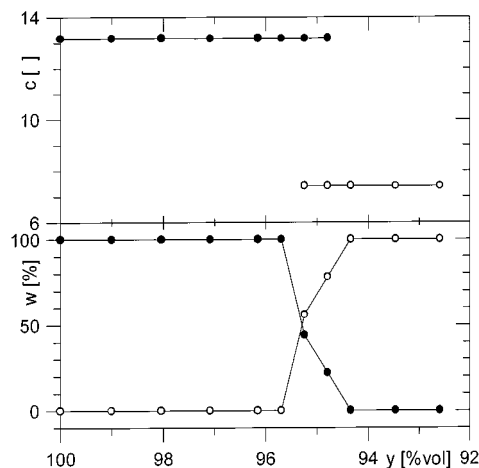


Figure 1. Basal spacing and content of the solid products in the VOPO_4 /water/ethanol system

without any occurrence of random stacking of the layers (Hendricks–Teller effect).

The dependence of the extent of reaction of dihydrate (α_H) and ethanol intercalate (α_E) on reaction time is shown in Figure 2. The reintercalation process starts very quickly. The kinetics curves do not have a sigmoidal shape. Their shape could probably be described as exponential or, better still, as a combination of parabolic and linear dependences. This type of kinetic curve has been found for some heterogeneous oxidations of metals with gaseous oxygen^[18–20] or during reactions of metals with sulfur vapors.^[21–23] This type of reaction is supposed to be a two-step process. In our case, the first step may involve replacement of the water molecules by ethanol and the second step could be a rearrangement of the ethanol molecules to form bilayers in the interlayer space. This idea is supported by the existence of the non-diffracting phase, which separates pristine and intercalated parts of the crystals as an advanced phase boundary.^{[15][24]} In this very disordered zone of the crystals, the host layers are bent so that segments with variable interlayer distance containing a mixture of both guests are formed. In addition, interlayer spaces filled with water or ethanol molecules can vary along the c axis in this zone. The amount of this non-diffracting phase corresponds to a difference of $\alpha_H - \alpha_E$, which is shown in Figure 2 (open circles). This phase is formed very quickly and then slowly transforms to the product during the reaction.

A progressive hydration of the intercalate $\text{VOPO}_4 \cdot 2\text{C}_2\text{H}_5\text{OH}$ was studied by XRD at several relative humidities (r.h.). The course of hydration is similar for relative humidities lower than 75%. The exchange of ethanol molecules for water is also fast and the reaction time depends on the relative humidity used and sample thickness. The lines observed in the diffractograms belong to either vanadyl phosphate dihydrate or ethanol-intercalated vanadyl phosphate, indicating that, as in the reaction of $\text{VOPO}_4 \cdot 2\text{H}_2\text{O}$ with ethanol, there is no crystalline intermediate product such as $\text{VOPO}_4 \cdot \text{C}_2\text{H}_5\text{OH} \cdot \text{H}_2\text{O}$. All diffraction lines (00 l) are sharp and their positions do not change.

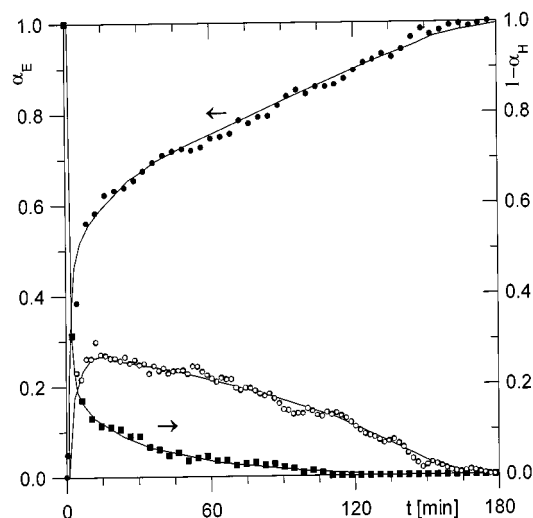


Figure 2. Dependence of the extent of reaction of the parent vanadyl phosphate dihydrate α_H and the product α_E on time t obtained by XRD during reintercalation of $\text{VOPO}_4 \cdot 2\text{H}_2\text{O}$ with ethanol vapours; the difference $\alpha_H - \alpha_E$ (open circles) corresponds to the amount of non-diffracting phase

The dependence of the extent of reaction of ethanol intercalate and dihydrate at r.h. = 11% on the reaction time is shown in Figure 3. The shape of the kinetic curves is very similar to those in the case of the formation of ethanol intercalate and, indeed, a similar mechanism is presumed to be operating. The formation of non-diffracting phases was also observed.

A different course of reaction was observed at high humidities. Changes in the diffractograms during hydration at 92% r.h. are shown in Figure 4. The ethanol intercalate is transformed to vanadyl phosphate pentahydrate (basal spacing 10.5 Å) very quickly. The intensity of the series of three (001) lines of $\text{VOPO}_4 \cdot 5\text{H}_2\text{O}$ decreases during hydration and the dihydrate is formed. This process is supported by two factors: the large interlayer distance in

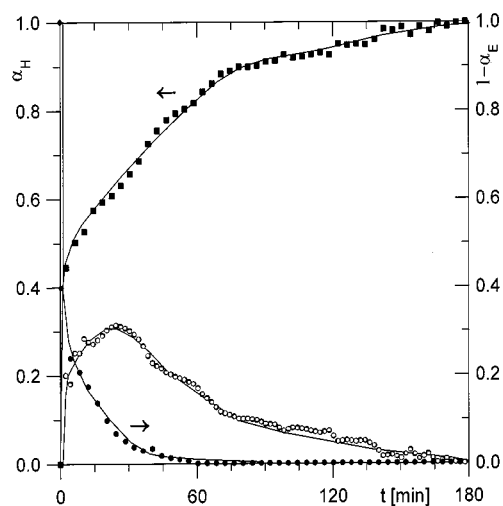


Figure 3. Dependence of the extent of reaction of the ethanol intercalate α_E and the product α_H on time t obtained by XRD during hydration of the ethanol intercalate at 11% r.h.; the difference $\alpha_H - \alpha_E$ (open circles) corresponds to the amount of non-diffracting phase

$\text{VOPO}_4 \cdot 2\text{C}_2\text{H}_5\text{OH}$ (compared with $\text{VOPO}_4 \cdot 2\text{H}_2\text{O}$) and the high concentration of water molecules in air at 92% r.h. The attacking water molecules fill the interlayer space after the release of ethanol before the layers are able to move closer together. The unstable pentahydrate formed then slowly decomposes to the dihydrate.

FTIR Spectroscopy

IR spectra of $\text{VOPO}_4 \cdot 2\text{C}_2\text{H}_5\text{OH}$ and its spectra upon progressive hydration by atmospheric water are shown in Figure 5 together with the spectrum of pure ethanol. One can easily identify the bands corresponding to the ethanol molecules. The ethanol bands maintain the same position in the IR spectra of the intercalate as in pure ethanol. This

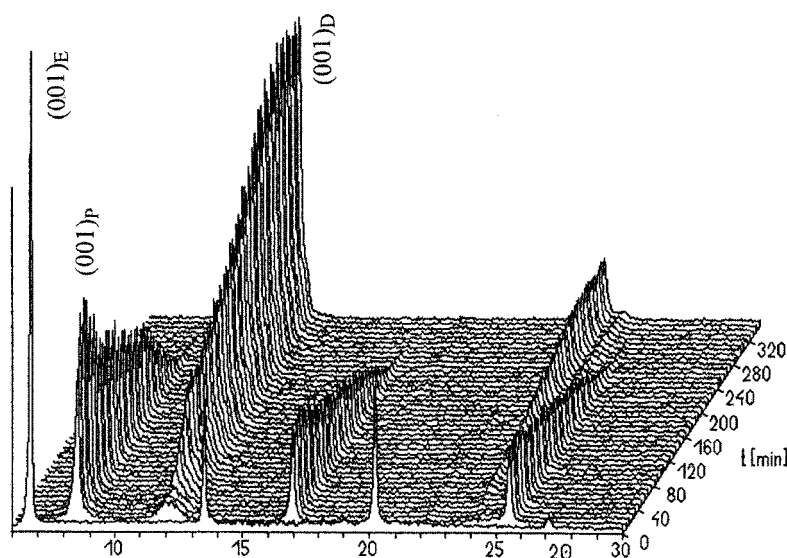


Figure 4. The changes of the diffractograms during hydration of $\text{VOPO}_4 \cdot 2\text{C}_2\text{H}_5\text{OH}$ at 92% r.h.

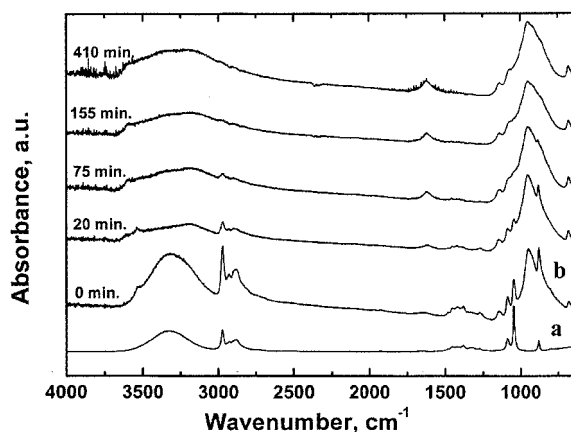


Figure 5. IR spectrum of pure ethanol (a) and $\text{VOPO}_4 \cdot 2\text{C}_2\text{H}_5\text{OH}$ (b) as a function of time of hydration by atmospheric water molecules

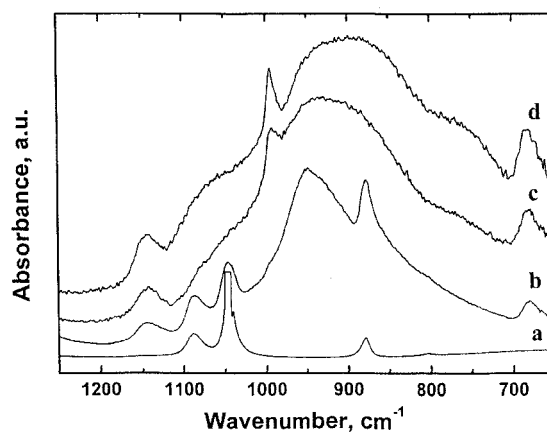


Figure 6. IR spectra of pure ethanol (a), $\text{VOPO}_4 \cdot 2\text{C}_2\text{H}_5\text{OH}$ (b), this intercalate upon 24 hours of hydration by atmospheric water (c) and $\text{VOPO}_4 \cdot 2\text{H}_2\text{O}$ (d)

is due to the weak ethanol–layer bonding.^[25] IR spectra of $\text{VOPO}_4 \cdot 2\text{C}_2\text{H}_5\text{OH}$ and $\text{VOPO}_4 \cdot 2\text{H}_2\text{O}$ are given in Figure 6. In the IR spectra of the dihydrate and intercalate we can see the same bands at the same positions (see Table 1). The broadened band in the spectrum of the $\text{VOPO}_4 \cdot 2\text{H}_2\text{O}$ (with the center of gravity at about 920 cm^{-1}) contains a mixture of overlapping bands: $\nu_1(\text{PO}_4)$, $\delta(\text{P}–\text{O}–\text{V})$ and $\rho(\text{H}_2\text{O})$. It is evident that this band changes its profile on going from $\text{VOPO}_4 \cdot 2\text{C}_2\text{H}_5\text{OH}$ to the dihydrate. Evidence for this is that $\rho(\text{H}_2\text{O})$ bands are absent and $\delta(\text{P}–\text{O}–\text{V})$ deformation bands are suppressed in the intercalate due to the smaller number of hydrogen bonds between ethanol and the host layers in comparison with the network of hydrogen bonds in $\text{VOPO}_4 \cdot 2\text{H}_2\text{O}$. The band due to the degenerate asymmetric stretching vibration $\nu_3(\text{PO}_4)$ is active only in the IR spectra and its position at 1143 cm^{-1} is the same as in the intercalate. Only one band of a stretching $\text{V}=\text{O}$ vibration is observed in the spectra of $\text{VOPO}_4 \cdot 2\text{C}_2\text{H}_5\text{OH}$ and $\text{VOPO}_4 \cdot 2\text{H}_2\text{O}$ and this occurs at the same position (995 cm^{-1}). The same is valid for the lattice vibration at 681 cm^{-1} .

In agreement with other authors^[26] we believe that the sharp bands near 3600 and 1620 cm^{-1} in the spectrum of

$\text{VOPO}_4 \cdot 2\text{H}_2\text{O}$ (see Figure 5) are due to strongly bonded water molecules within the crystalline lattice associated with the water molecule bound to vanadium. The additional lattice water is indicated by the broad bands near 3300 and 1620 cm^{-1} in the spectrum of the dihydrate. In the bending vibration at 1620 cm^{-1} , sharp and broad bands are superimposed. In the spectrum of intercalate at the beginning of the hydration process (0 min.) we can assign the sharp bands near 3600 cm^{-1} to the ethanol molecule that is strongly bonded to vanadium (this peak is absent in the spectrum of pure ethanol). The broad band at 3350 cm^{-1} corresponds to the stretching vibration of OH groups in ethanol molecules.

During the hydration process of $\text{VOPO}_4 \cdot 2\text{C}_2\text{H}_5\text{OH}$ in air the ethanol vibration bands gradually disappear and the bands corresponding to the water molecules in $\text{VOPO}_4 \cdot 2\text{H}_2\text{O}$ appear. After 24 hours of exposure to air the IR spectrum of the intercalate had completely changed to give the IR spectrum of the dihydrate (see Figure 6). Intermediate phases were not observed during the hydration process of $\text{VOPO}_4 \cdot 2\text{C}_2\text{H}_5\text{OH}$.

Table 1. Infrared (IR) and Raman (Ra) frequencies (cm^{-1}) of $\text{VOPO}_4 \cdot 2\text{H}_2\text{O}$ and $\text{VOPO}_4 \cdot 2\text{C}_2\text{H}_5\text{OH}$ (c.g.: center of gravity; s: strong; w: weak; sh: shoulder)

Vibration	$\nu_1(\text{PO}_4)$ symmetric stretching	$\nu_2(\text{PO}_4)$ symmetric bending	$\nu_3(\text{PO}_4)$ asymmetric stretching	$\nu_4(\text{PO}_4)$ asymmetric bending	lattice	$\text{V}=\text{O}$ stretching	$\nu_2(\text{H}_2\text{O})$	$\nu_1(\text{H}_2\text{O})$
$\text{VOPO}_4 \cdot 2\text{H}_2\text{O}$								
IR	c.g. 920	Not observable	1143 1076 w	Not observable	681	995	3130 3310 3500 sh 3600 sh	1615
Ra	945 s 929 sh	460 433	Not observable	579 541	Inactive	1035 985	Inactive	—
$\text{VOPO}_4 \cdot 2\text{C}_2\text{H}_5\text{OH}$								
IR	c.g. 920	Not observable	1143 Et. band ov.	Not observable	681	995	3350 3600	—
Ra	937 s	—	1147	591 542	Inactive	1029 990	Inactive	—

Raman Spectroscopy

The Raman spectra of anhydrous VOPO_4 , $\text{VOPO}_4 \cdot 2\text{C}_2\text{H}_5\text{OH}$, the intermediate states obtained by hydration with atmospheric water, and $\text{VOPO}_4 \cdot 2\text{H}_2\text{O}$ are shown in Figure 7. The ethanol bands in the Raman spectrum of $\text{VOPO}_4 \cdot 2\text{C}_2\text{H}_5\text{OH}$ are in exactly the same positions as in the spectrum of pure ethanol. Consequently, the ethanol spectrum can be subtracted from the spectrum of the intercalate. As a result of this subtraction we obtained the spectrum of the intercalate without ethanol bands, which is more convenient for the comparison of bands corresponding to the VOPO_4 layers in the dihydrate, anhydrous, and intercalated structure. The most intense band of the Raman spectrum, with a maximum at about 929 cm^{-1} in the anhydrous form, at 937 cm^{-1} in $\text{VOPO}_4 \cdot 2\text{C}_2\text{H}_5\text{OH}$, and at 945 cm^{-1} in $\text{VOPO}_4 \cdot 2\text{H}_2\text{O}$, corresponds to the symmetric stretching vibration $\nu_1(\text{PO}_4)$. This band is especially active in the Raman spectra. The bands of the degenerate asymmetric stretching vibration $\nu_3(\text{PO}_4)$ are not observed in the Raman spectra. In addition, the bands due to symmetric bending vibrations [$\nu_4(\text{PO}_4)$ at 579 cm^{-1} and 541 cm^{-1}] and bands due to asymmetric bending vibrations [$\nu_2(\text{PO}_4)$ at 460 and 433 cm^{-1}] are observed in the Raman spectra of the samples. Two bands can be observed at 1029 and 990 cm^{-1} in the Raman spectrum of the host structure and these correspond to the $\text{V}=\text{O}$ stretching mode. The vanadyl stretching band is especially sensitive to the local coordination of vanadium and two peaks indicate the presence of anhydrous and hydrated forms of VOPO_4 . Only one peak at 1036 cm^{-1} is observed in the anhydrous form. The partial escape of water in the hydrated form is due to the heating caused by a laser beam during the measurements (for a detailed explanation see ref. [12]). In the case of $\text{VOPO}_4 \cdot 2\text{C}_2\text{H}_5\text{OH}$, these bands are slightly shifted and broadened. This broadening of $\text{V}=\text{O}$ stretching bands reflects the disorder in the position of ethanol molecules found by molecular simulations. [25] The irregularity in hydrogen bonding of ethanol to PO_4 oxygen atoms also affects the PO_4 stretching and bending modes.

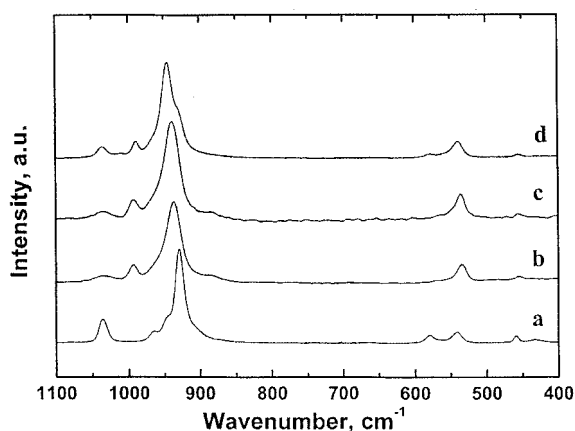


Figure 7. Raman spectra of anhydrous VOPO_4 (a), $\text{VOPO}_4 \cdot 2\text{C}_2\text{H}_5\text{OH}$ (b), the intermediate state of hydration (c) and $\text{VOPO}_4 \cdot 2\text{H}_2\text{O}$ (d). The ethanol spectrum was subtracted from the spectrum of $\text{VOPO}_4 \cdot 2\text{C}_2\text{H}_5\text{OH}$

Conclusions

A progressive hydration of $\text{VOPO}_4 \cdot 2\text{C}_2\text{H}_5\text{OH}$ has been studied by X-ray analysis and ATR FTIR and Raman spectroscopy. The mixed intercalate $\text{VOPO}_4 \cdot \text{C}_2\text{H}_5\text{OH} \cdot \text{H}_2\text{O}$ is not formed during hydration of $\text{VOPO}_4 \cdot 2\text{C}_2\text{H}_5\text{OH}$. During this hydration, only vanadyl phosphate dihydrate or pentahydrate (at high relative humidity) are formed. In contrast to the intercalation of ethanol into anhydrous vanadyl phosphate, the kinetic curves of reintercalation of dihydrate do not have a sigmoidal shape. The shape of the kinetic curve indicates a transition of at least one reaction zone through the crystal. A similar course is also observed for the reintercalation of $\text{VOPO}_4 \cdot 2\text{H}_2\text{O}$ with ethanol. A delay in the formation of the product in comparison with the decrease in the amount of starting material is explained by the existence of very disordered phase.

The reintercalation reactions are very fast and their activation energy is presumed to be very low compared with that of intercalation of water or ethanol into anhydrous VOPO_4 . This is due to the sufficient interlayer distance in the starting materials. Moreover, no energy is needed for $\text{V}=\text{O} \cdots \text{V}$ bond breaking, as is seen in the case of intercalation into anhydrous VOPO_4 . [14] As inferred from the constant position of the stretching $\text{V}=\text{O}$ vibration during hydration of $\text{VOPO}_4 \cdot 2\text{C}_2\text{H}_5\text{OH}$, both guests are anchored to the host layers by similar bonds and therefore no large change in the bond energy is expected during the reaction.

Experimental Section

The samples of $\text{VOPO}_4 \cdot 2\text{C}_2\text{H}_5\text{OH}$ for the IR and Raman measurements were prepared by suspending solid $\text{VOPO}_4 \cdot 2\text{H}_2\text{O}$ in dry ethanol for two hours. After filtration, the product was dried in nitrogen and kept in sealed ampoules. The study of the equilibration in the VOPO_4 /ethanol/water system was carried out by contacting $\text{VOPO}_4 \cdot 2\text{H}_2\text{O}$ or $\text{VOPO}_4 \cdot 2\text{C}_2\text{H}_5\text{OH}$ (0.25 g) with 10 mL of ethanol/water mixture (from 92.5 to 100 vol% of ethanol) for two hours. The powder data of the intercalates with a small excess of the guest were obtained with an X-ray diffractometer HZG-4 (Präzisionsmechanik, Germany) using Cu-K_α radiation with discrimination from Cu-K_β by a Ni-filter. The exchange reactions were performed in the following way: the sample of $\text{VOPO}_4 \cdot 2\text{H}_2\text{O}$ or $\text{VOPO}_4 \cdot 2\text{C}_2\text{H}_5\text{OH}$ was placed on the surface of a thermostated (25°C) corundum target plate under dry nitrogen, whereupon the stream (ca. 0.5 L min^{-1}) of nitrogen saturated with vapors of ethanol or water was introduced onto the sample. The reaction taking place in the solid phase was monitored by recording the diffractograms (from $6 < 2\theta < 30$) at 8 minute intervals. The intensities of the (001) reflections of $\text{VOPO}_4 \cdot 2\text{H}_2\text{O}$ and $\text{VOPO}_4 \cdot 2\text{C}_2\text{H}_5\text{OH}$ were obtained from diffractograms measured from $5.5 < 2\theta < 15$ at 4 minute intervals. The extent of reaction, α_p , for the product at time t is given by the equation:

$$\alpha_p = B/B_\infty$$

where B is the intensity of the (001) line of the product at time t and B_∞ is this intensity at infinite time. Analogously, the equation:

$$\alpha_s = 1 - A/A_0$$

describing the extent of the reaction, α_s , for the decrease in the amount of the starting material at time t can be defined, where A

is the intensity of the (001) line of the starting material at time t and A_0 is this intensity at time $t = 0$. Depending on the direction of the reaction, $a_P = a_E$ and $a_S = a_H$ when the starting material is dihydrate, whereas $a_P = a_H$ and $a_S = a_E$ when the starting material is the ethanol intercalate.

Infrared measurements were carried out using a NICOLET IMPACT 400 Fourier transform infrared (FTIR) spectrophotometer in an H₂O-purged environment. An ambient-temperature deuterated triglycine sulfate (DTGS) detector was used for the wavelength range from 400 to 4000 cm⁻¹. A Happ-Genzel apodization function was used in the whole region and the spectral resolution was 2 cm⁻¹. Approximately 300 scans were coadded to achieve the signal-to-noise ratio shown. The Baseline Horizontal Attenuated Total Reflection (ATR) accessory with ZnSe crystal ($n = 2.4$ at 1000 cm⁻¹) was used for measurements of infrared spectra of the samples. In our experiments the effective path length was approximately a few μm (angle of incidence = 60°, number of reflections = 7). The ATR correction was performed in order to eliminate the dependence of the effective path length on the wavelength. After some trials it was found that the best results were obtained, if a sample is exposed for a definite time to the external conditions without removing the sample from the crystal between the subsequent spectral measurements. In this situation the water molecules arrive at the surface of the ZnSe crystal from the bulk volume and the adsorption of water at the measured surface of the sample is avoided.

FT Raman spectra were collected using an Equinox 55/S Fourier transform near-infrared (FT-NIR) spectrometer (Bruker) equipped with FT Raman module FRA 106/S (Bruker). The samples were irradiated by the focused laser beam (power 100 mW) of an Nd-YAG laser (1064 nm, Coherent). The scattered light was collected in backscattering geometry. A quartz beamsplitter and Ge detector (liquid N₂ cooled) were used to obtain interferograms. 128 interferograms were co-added and then processed by Fourier transformation with Blackman-Harris 4-term apodization and a zero-filling factor of 8 to obtain final FT Raman spectra in the range 4000–1000 cm⁻¹ with 4 cm⁻¹ resolution.

The FT Raman spectra of pure species (VOPO₄, VOPO₄·2H₂O, VOPO₄·2C₂H₅OH) were obtained from samples in sealed glass ampoules. In each case the glass ampoule was placed in the sample holder and aligned by the motorized x-y-z sample stage to achieve the optimal optical condition of irradiation of the sample and of the collection of the scattered light. The FT Raman spectra collected during the intercalation of water were obtained from the samples placed in the aluminium cup. The aluminium cup was optically pre-aligned using sulfur as a sample, and then sulfur was replaced by the particular sample studied.

Acknowledgments

We are grateful to Professor J. Votinský from University of Pardubice for fruitful discussions and Professor B. Strauch from Charles University for help with interpretation of spectra. This work was supported by the Grant Agency of the Czech Republic, grant no: 203/97/1010 and Grant Agency GAUK, grant no: 37/97/B.

- [1] H. R. Tietze, *Aust. J. Chem.* **1981**, *34*, 2035–2038.
- [2] M. Tachez, F. Theobald, J. Bernard, A. W. Hewat, *Rev. Chim. Minerale* **1982**, *19*, 291–300.
- [3] J. Kalousová, J. Votinský, L. Beneš, K. Melánová, V. Zima, *Collect. Czech. Chem. Commun.* **1998**, *63*, 1–19.
- [4] K. Beneke, G. Lagaly, *Inorg. Chem.* **1983**, *22*, 1503–1507.
- [5] L. Beneš, R. Hyklová, J. Kalousová, J. Votinský, *Inorg. Chim. Acta* **1990**, *177*, 71–74.
- [6] N. Kinomura, T. Toyama, N. Kumada, *Solid State Ionics* **1995**, *78*, 281–286.
- [7] J. W. Johnson, A. J. Jacobson, J. F. Brody, S. M. Rich, *Inorg. Chem.* **1982**, *21*, 3820–3825.
- [8] L. Beneš, K. Melánová, V. Zima, J. Kalousová, J. Votinský, *Inorg. Chem.* **1997**, *36*, 2850–2853.
- [9] L. Beneš, J. Votinský, J. Kalousová, K. Handlíř, *Inorg. Chim. Acta* **1990**, *176*, 255–259.
- [10] M. Martínez-Lara, L. Moreno-Real, A. Jimenez-Lopez, S. Bruque-Gamez, A. Rodriguez-Garcia, *Mat. Res. Bull.* **1986**, *21*, 13–23.
- [11] L. Beneš, V. Zima, *J. Incl. Phenom.* **1995**, *20*, 381–391.
- [12] M. Trchová, P. Čapková, K. Melánová, L. Beneš, P. Matějka, *J. Solid State Chem.* in press.
- [13] L. Beneš, J. Votinský, J. Kalousová, J. Klikorka, *Inorg. Chim. Acta* **1986**, *114*, 47–50.
- [14] L. Beneš, V. Zima, I. Baudyšová, J. Votinský, *J. Incl. Phenom.* **1996**, *26*, 311–319.
- [15] G. Alberti, *Acc. Chem. Res.* **1978**, *11*, 163–170.
- [16] P. Čapková, D. Janeba, L. Beneš, K. Melánová, H. Schenk, *J. Mol. Model.* **1998**, *4*, 150–157.
- [17] G. Matsubayashi, S. Ohta, *Chem. Lett.* **1990**, 787–790.
- [18] G. Valensi, *J. Chim. Phys.* **1950**, *47*, 489–505.
- [19] W. W. Webb, J. J. Norton, C. Wagner, *J. Electrochem. Soc.* **1956**, *103*, 107–111.
- [20] W. B. Jepson, D. W. Almore, *J. Electrochem. Soc.* **1961**, *108*, 942–947.
- [21] M. Billy, G. Valensi, *J. Chim. Phys.* **1956**, *53*, 832–844.
- [22] I. Czerski, S. Mrowec, T. Werber, *J. Electrochem. Soc.* **1962**, *109*, 273–278.
- [23] J. C. Colson, D. Delafosse, P. Barret, *Bull. Soc. Chim. Fr.* **1968**, *1*, 146–154.
- [24] L. Beneš, K. Melánová, V. Zima, J. Kalousová, J. Votinský, *J. Incl. Phenom.* **1998**, *31*, 275–286.
- [25] P. Čapková, M. Trchová, P. Matějka, J. Votinský, H. Schenk, *J. Mol. Model.* **1998**, *4*, 284–293.
- [26] M. R. Antonio, R. L. Barbour, P. R. Blum, *Inorg. Chem.* **1987**, *26*, 1235–1243.

Received May 28, 1999
[199198]